Optica Applicata, Vol. XL, No. 1, 2010

Red up-conversion dynamics in Er^{3+}-doped TeO_2–ZnO glasses

ABDELFATTEH CHERIF*, ABDELAZIZ KANOUN, NEJEH JABA

Laboratoire de Physique des Semi-conducteurs, Département de Physique, Faculté des Sciences, 5019 Monastir, Tunisie

*Corresponding author: cherif_af@yahoo.fr

Red fluorescence has been obtained under 980 nm excitation in Er^{3+}-doped TeO_2–ZnO glasses. The dynamics of the red up-conversion is well explained with the proposed model. The energy transfer processes are predominant.

Keywords: tellurite glasses, erbium: Er^{3+}, dynamics of up-conversion.

1. Introduction

Rare earth-activated fluoride and oxide glasses are very attractive materials for many applications, such as optical amplifiers in the second and third telecommunications windows (at 1.3 and 1.53 μm, respectively) and frequency up-converters [1, 2]. One of the most used oxide glasses is tellurite thanks to its good compromise between high refractive index and low oxide phonon energy [3, 4]. Rare-earth doped solids materials have been studied by the up-conversion [5]. In addition, this phenomenon (up-conversion) has been used to explain laser processes [6]. In the rare-earth doped glasses, the emission always occurs at 4*f* electron level. Their up-conversion can be understood by the well-known mechanisms [6–14]: excited-state absorption (ESA), energy transfer up-conversion (ETU) and photon avalanche (PA).

The up-conversion fluorescence has already been studied in Er^{3+}-doped TeO_2–Na_2O [15], TeO_2–PbO [16], TeO_2–ZnO [17] and TeO_2–Nb_2O_5 [18].

In this paper, we present an analysis of Er^{3+} optical transitions behavior in the visible range. We have focused our study details on the red emission centered on 670 nm. Finally, we have investigated the dynamics of the $^4F_{9/2}$ state and explained it based on the relative efficiency of the different mechanisms.

2. Experimental details

Glasses were prepared from oxide powders of TeO_2, ZnO and Er_2O_3 as starting materials using the conventional melt-quenching method. The amount of dopant was

varied between 0.2 and 3 mol% Er_2O_3. A continuous wave infrared Ti:saphire laser tuned to 980 nm was used for up-conversion excitation in the 400–700 nm regions. The intrinsic lifetimes of the levels were obtained by exciting the samples with a laser analytical systems dye laser pumped by a pulsed frequency doubled Nd:YAG laser from BM Industries. The duration of pulses was 8 ns. The emitted light has been focused on a Jobin–Yvon HR S2 spectrophotometer. The detection has been performed using an R 1767 Hammamatsu photomultiplier and a Lecroy 9410 averager oscilloscope. All experiments were performed at room temperature.

3. Up-conversion results and mechanisms

Figure 1 shows the up-conversion spectra of Er^{3+}-doped samples (0.2 and 3 mol%) excited at 980 nm. As we can note, the luminescence intensities increase with increasing Er^{3+} content. The emission bands associated with Er^{3+} transitions are centered at 410 nm ($^2H_{9/2} \rightarrow {}^4I_{15/2}$), 530 nm ($^4H_{11/2} \rightarrow {}^4I_{15/2}$), 555 nm ($^4S_{3/2} \rightarrow {}^4I_{15/2}$) and 670 nm ($^4F_{9/2} \rightarrow {}^4I_{15/2}$). The green emission at 555 nm is more efficient than the red one at 670 nm. The blue $^2H_{9/2} \rightarrow {}^4I_{15/2}$ up-conversion transition around 410 nm has been barely observed.

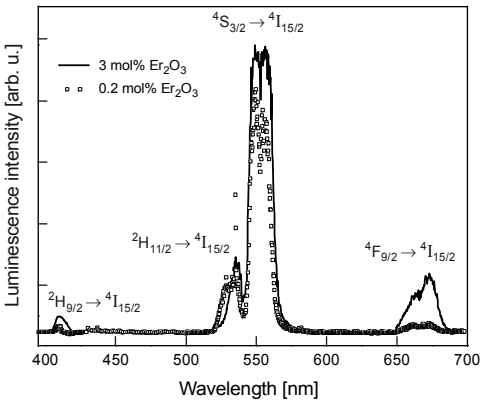

Fig. 1. Up-conversion spectra for 0.2 and 3 mol% Er^{3+} in the $70TeO_2$–30ZnO tellurite glass at $T = 300$ K, of the blue, green and red emissions.

In our study, we focus our investigation on the emission line in the red region of the spectrum at 670 nm. As we can observe in Fig. 1, the intensity of the red up-conversion emission in the heavily doped sample remains much stronger than in the sample with low erbium concentration. If we consider that the excite-state absorption (ESA) is the only process responsible for the up-conversion in the case of the weak concentrations of dopant, this result means that ESA cannot explain the weaker signal obtained for 0.2 mol% erbium (at 670 nm). Also, the red up-conversion for 3 mol% erbium is not explained by ESA, since this process does not depend on the concentration.

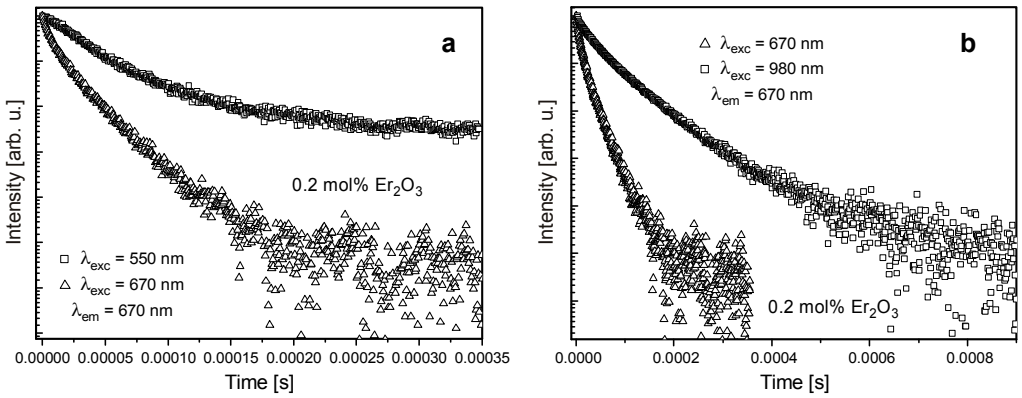

Fig. 2. Luminescence decays from ${}^4F_{9/2} \rightarrow {}^4I_{15/2}$, for two excitations: λ_{exc} = 550 nm (square) and λ_{exc} = 670 nm (triangle) – **a**, and λ_{exc} = 980 nm (square) and λ_{exc} = 670 nm (triangle) – **b**, for weakly concentrated samples (0.2 mol%).

In order to confirm this assumption, we have recorded the luminescence decays of the transition ${}^4F_{9/2}$ after direct (λ_{exc} = 670 nm) and under two selective laser pulse excitations (at λ_{exc} = 980 nm and λ_{exc} = 550 nm), for 0.2 mol% concentration. Figure 2**a** shows a difference in decay profiles of the red emission (at λ_{exc} = 670 nm and λ_{exc} = 550 nm). This result means that the ${}^4F_{9/2}$ level cannot be populated via a non-radiative relaxation through the ${}^4S_{3/2}$ excited state.

Furthermore, Fig. 2**b** shows that luminescence decay is different for both λ_{exc} = = 980 nm and λ_{exc} = 670 nm. These results imply that the excite-state absorption is not responsible for red up-conversion. The dominant mechanism is then the energy transfer up-conversion (ETU).

To better understand the up-conversion mechanism, we have measured the luminescence intensity of red emission as a function of the pump power. Figure 3 exhibits

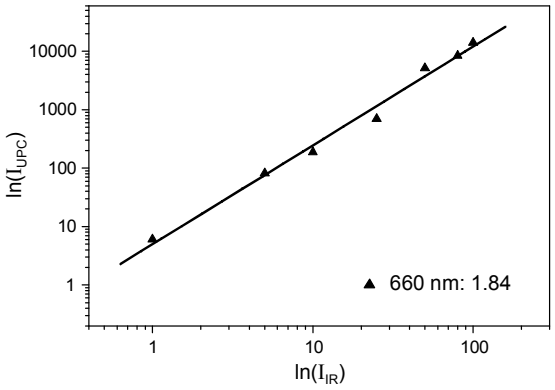

Fig. 3. Intensity of the up-converted red emission from Er^{3+} versus laser power excitation, for 3 mol% Er^{3+} in tellurite glass using 980 nm excitation. Measurements were performed at 300 K. The value 1.84 is the slope of the line.

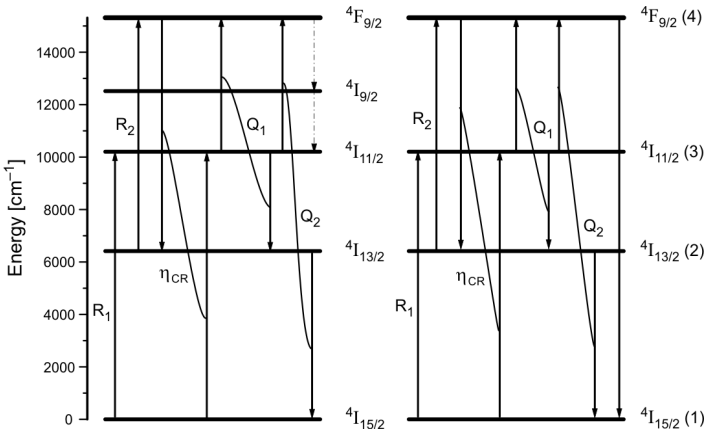

Fig. 4. Energy transfer and up-conversion processes considered in the model proposed in this work to explain the dynamics of the active ions in TeO_2–ZnO:Er^{3+} glass.

a log–log plot of I_{upc} versus I_{IR} intensities. As we can note, we have obtained a linear behavior. The extracted slope is about 1.84. This indicates that the red emission arises from a two-step up-conversion process.

Figure 4 illustrates the energy level diagram. In this figure, the possible mechanisms leading to the observed red luminescence after infrared excitation are also shown. The excited $^4F_{9/2}$ state can be populated by two possible mechanisms, ESA and/or energy transfer (ETU). In the first process (ESA), one Er^{3+} ion, initially in the ground state, absorbs one IR photon and is excited to the $^4I_{11/2}$ state from where the $^4I_{13/2}$ state is populated by multiphonon relaxation. This is followed by the absorption of a second IR photon from the $^4I_{13/2}$ excited state to the $^4F_{9/2}$ state. In the second process (ETU), we can explain the up-conversion of the red emitting $^4F_{9/2}$ state by three mechanisms:

– The first one is the energy transfer up-conversion ETU-1: $^4I_{11/2} + {}^4I_{11/2} \rightarrow$ $\rightarrow {}^4I_{13/2} + {}^4F_{9/2}$.

– The second one is the energy transfer up-conversion ETU-2: $^4I_{13/2} + {}^4I_{11/2} \rightarrow$ $\rightarrow {}^4I_{15/2} + {}^4F_{9/2}$.

– The third one is the ESA: $^4I_{13/2} \rightarrow {}^4F_{9/2}$.

And of the cross-relaxation (RC): $^4I_{15/2} + {}^4F_{9/2} \rightarrow {}^4I_{13/2} + {}^4I_{11/2}$.

3.1. Decay times investigation

The evidence of excitation-density-dependent decay is most easily presented through the use of luminescence decay measurements.

Lifetimes of $^4I_{11/2}$ and $^4F_{9/2}$ transitions, into direct excitations, show non-exponential behaviors which can be fitted by a mean decay lifetime given by:

$$\tau_m = \int_0^\infty \frac{I(t)}{I_0} \mathrm{d}t$$

In case of $^4I_{13/2}$ the decay transient was fitted with the dual exponential decay function:

$$\frac{I(t)}{I(0)} = \exp\left(-\frac{t}{\tau_1}\right) - \exp\left(-\frac{t}{\tau_2}\right)$$

where τ_1 and τ_2 are the decay times of $^4I_{11/2}$ and $^4I_{13/2}$, respectively.

The values of measured lifetimes for different Er^{3+} ion concentrations ranging from 0.5 to 3 mol% are gathered in Tab. 1.

T a b l e 1. Values of measured lifetimes τ_{mes} of different levels and the cross-relaxation energy transfer efficiency η_{CR} of $^4F_{9/2}$ state for 0.5, 1 and 3 mol% Er^{3+}.

Er_2O_3 [mol%]	0	0.5	1	3
$\tau_{^4I_{13/2}}$ [μs]	2600	2488	1666	1499
$\tau_{^4I_{11/2}}$ [μs]	145	132	114	86
$\tau_{^4F_{9/2}}$ [μs]	28	25	12	10
$\eta_{CR}(^4F_{9/2})$	0	0.11	0.51	0.64

The cross-relaxation energy transfer efficiency η_{CR} for an active ion concentration of c% may be derived from the fluorescence decays using the following equation:

$$\eta_{CR} = 1 - \frac{\int_0^\infty I_{(c\%)}\,\mathrm{d}t}{\tau_{(0\%)}}$$

The integral determines the area under the fluorescence decay curves. The results given in Tab. 1 show really high cross-relaxation energy transfer efficiencies in the 3 mol% Er^{3+} doped TeO_2–ZnO glass. Several articles use this definition to determine the quantum yield of the cross-relaxation mechanism [19–21].

3.2. Up-conversion investigation

The evaluations of the radiative lifetimes are indeed required to understand deexcitation mechanisms. To evaluate the radiative decay rate of the different transitions, the intensity parameters $\Omega_{t=2,4,6}$ have been calculated using the Judd–Ofelt formulae [22, 23]. The relevant values are $\Omega_2 = 5.93\times10^{-20}$ cm^2, $\Omega_4 = 1.50\times10^{-20}$ cm^2, and $\Omega_6 = 1.07\times10^{-2}$ cm^2 [24]. From these parameters, the branching ratio β_{ij} of the (ij) transition and the radiative lifetimes can be evaluated.

The corresponding radiative lifetimes (Tab. 2) were compared with the measured lifetimes of the $^4F_{9/2}$, $^4I_{11/2}$ and $^4I_{13/2}$ levels. The $^4F_{9/2} \rightarrow {}^4I_{9/2} \rightarrow {}^4I_{11/2}$ transitions are mainly non-radiative and their quantum yields are almost l00%, so the $^4I_{9/2}$ level is not retained in the model.

T a b l e 2. Values of radiative lifetimes τ_r of different levels for 0.5, 1 and 3 mol% Er^{3+}.

Level	$\tau_{^4I_{13/2}}$ [μs]	$\tau_{^4I_{11/2}}$ [μs]	$\tau_{^4F_{9/2}}$ [μs]
Radiative lifetime	3535	2850	325

T a b l e 3. Values of the parameters used in our model.

τ_2 [μs]	τ_3 [μs]	τ_4 [μs]	β_{32} [%]	β_{42} [%]	β_{43} [%]	η_{CR} [%]
2600	145	28	16.0	4.9	5.0	64

The ground state absorption from the $^4I_{15/2}$ level to the $^4I_{11/2}$ level is represented by arrow R_1 ($1 \rightarrow 3$) and the transition $^4I_{13/2} \rightarrow {}^4F_{9/2}$ is represented by the arrow R_2 ($2 \rightarrow 4$). The parameters of the model are gathered in Tab. 3.

ESA process is a single ion process and is independent of Er^{3+} ions concentration, while ETU process involves two ions. Therefore the up-converted luminescence intensity in the ETU process usually varies quadratically with the dopant rare-earth ions concentration [6, 19, 25–30].

We are ready to exhibit a model, to describe the dynamics of the red up-conversion. Discussions of different models are presented in the literature [31–40].

Theoretically, the system can be easily described by a four levels scheme (at $\lambda_{exc} = 980$ nm). Our model is expressed by the following population rate equations:

$$\frac{dn_2}{dt} = R_2 n_2 - \frac{n_2}{\tau_2} + \frac{\eta_{CR} n_1 n_4}{(1-\eta_{CR})\tau_4} + \frac{\beta_{32} n_3}{(1-\eta_{CR})\tau_4} + \frac{\beta_{42} n_4}{(1-\eta_{CR})\tau_4} - Q_2 n_3 n_2 + Q_1 n_3^2 \tag{1a}$$

$$\frac{dn_3}{dt} = R_1 n_1 - \frac{n_3}{\tau_3} - Q_2 n_3 n_2 + \frac{\beta_{43} n_4}{(1-\eta_{CR})\tau_4} - 2Q_1 n_3^2 + \frac{\eta_{CR} n_1 n_4}{(1-\eta_{CR})\tau_4} \tag{1b}$$

$$\frac{dn_4}{dt} = R_2 n_2 - \frac{n_4}{\tau_4} - \frac{\eta_{CR} n_1 n_4}{(1-\eta_{CR})\tau_4} + Q_2 n_3 n_2 + Q_1 n_3^2 \tag{1c}$$

$$n_1 + n_2 + n_3 + n_4 = 1 \tag{1d}$$

where n_1, n_2, n_3 and n_4 are the populations of $^4I_{15/2}$, $^4I_{13/2}$, $^4I_{11/2}$ and $^4F_{9/2}$ levels, respectively; R_1 is the GSA probability and R_2 is the ESA probability; Q_1 and Q_2 are the ETU up-conversion coefficients; β_{ij} is the branching ratio of the (ij) transition, and η_{CR} is the cross relaxation rate according to Fig. 4. We have measured all these parameters and their following values are returned in Tab. 4.

T a b l e 4. Values of fitting parameters: R_1, R_2, Q_1 and Q_2.

R_1 [s^{-1}]	R_2 [s^{-1}]	Q_1 [s^{-1}]	Q_2 [s^{-1}]
258	0.12	0.6	28345

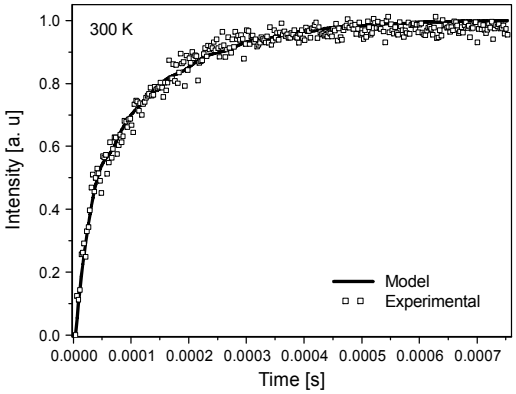

Fig. 5. Time evolution of the red fluorescence originating from the $^4F_{9/2}$ level at 980 nm excitation wavelength. The squares are the experimental data; the solid curve is the prediction of our model.

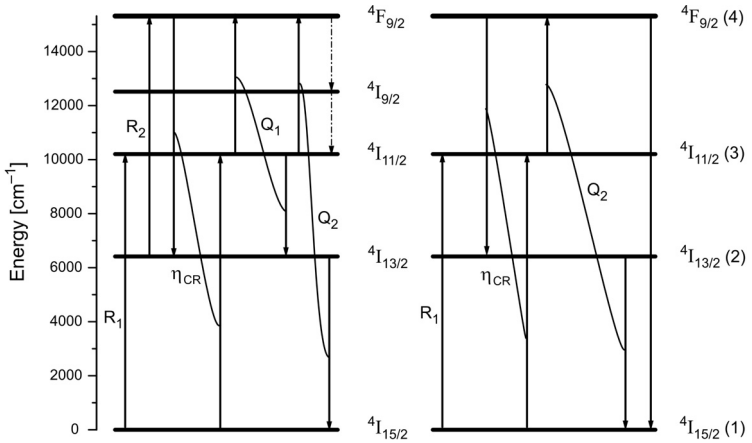

Fig. 6. Energy transfer and up-conversion processes considered in the simplified model.

System (1) leads to the fit of the time evolution of the red fluorescence represented by the line in Fig. 5 (at 980 nm). The fit was performed with four fitting parameters: R_1, R_2, Q_1 and Q_2.

Table 4 compares the numerical values for Er^{3+}-doped tellurite glass, and it can be seen that ASE and ETU-1 are insignificant. Therefore, we can simplify our model as presented in Fig. 6. In this situation, the population rate Eqs. (1) become:

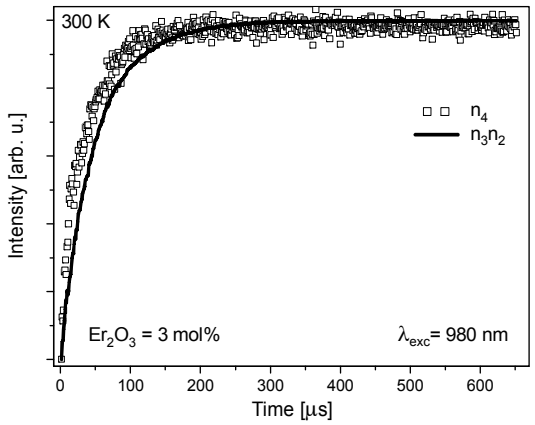

Fig. 7. Population change of level 4 is similar to that of population of levels 2 and 3.

$$\frac{\mathrm{d}n_2}{\mathrm{d}t} = -\frac{n_2}{\tau_2} + \frac{\eta_{\mathrm{CR}} n_1 n_4}{(1-\eta_{\mathrm{CR}})\tau_4} + \frac{\beta_{32} n_3}{(1-\eta_{\mathrm{CR}})\tau_4} + \frac{\beta_{42} n_4}{(1-\eta_{\mathrm{CR}})\tau_4} - Q_2 n_3 n_2 \tag{2a}$$

$$\frac{\mathrm{d}n_3}{\mathrm{d}t} = R_1 n_1 - \frac{n_3}{\tau_3} - Q_2 n_3 n_2 + \frac{\beta_{43} n_4}{(1-\eta_{\mathrm{CR}})\tau_4} + \frac{\eta_{\mathrm{CR}} n_1 n_4}{(1-\eta_{\mathrm{CR}})\tau_4} \tag{2b}$$

$$\frac{\mathrm{d}n_4}{\mathrm{d}t} = -\frac{n_4}{\tau_4} - \frac{\eta_{\mathrm{CR}} n_1 n_4}{(1-\eta_{\mathrm{CR}})\tau_4} + Q_2 n_3 n_2 \tag{2c}$$

$$n_1 + n_2 + n_3 + n_4 = 1 \tag{2d}$$

Equation (2c) suggests that change population of level 4 is similar to that population of levels 2 and 3 ($\mathrm{d}n_4/\mathrm{d}t \propto n_2 n_3$). Figure 7 confirms this idea.

4. Conclusions

Up-conversion emission at 670 nm has been obtained in tellurite glasses doped with 3 mol% by excitation with 980 nm. The dynamics of the red up-conversion is well explained with the proposed model; from the results it is possible to distinguish the contribution of two ETU processes and tell which one is predominant. The 670 nm up-conversion emission presents maximum for the up-conversion efficiency at high concentration and at room temperature.

References

[1] TANABE S., YOSHII S., HIRAO K., SOGA N., *Upconversion properties, multiphonon relaxation, and local environment of rare-earth ions in fluorophosphate glasses*, Physical Review B **45**(9), 1992, pp. 4620–4625.

[2] TANABE S., HIRAO K., SOGA N., *Upconversion fluorescences of TeO_2- and Ga_2O_3-based oxide glasses containing Er^{3+}*, Journal of Non-Crystalline Solids **122**(1), 1990, pp. 79–82.

[3] PAN Z., MORGAN S.H., DYER K., UEDA A., LIU H., *Host-dependent optical transitions of Er^{3+} ions in lead–germanate and lead–tellurium–germanate glasses*, Journal of Applied Physics **79**(12),1996, pp. 8906–891.

[4] MICHEL J.C., MORIN D., AUZEL F., *Propriétés spectroscopiques et effet laser d'un verre tellurite et d'un verre phosphate fortement dopés en néodyme*, Revue de Physique Appliquée **13**(12), 1978, pp. 859–866.

[5] AUZEL F.E., *Materials and devices using double-pumped phosphors with energy transfer*, Proceedings of the IEEE **61**(6), 1973, pp. 758–786.

[6] SCHEPS R., *Upconversion laser processes*, Progress in Quantum Electronics **20**(4), 1996, pp. 271–358.

[7] AUZEL F., MEICHENIN D., PELLÉ F., GOLDNER P., *Cooperative luminescence as a defining process for RE-ions clustering in glasses and crystals*, Optical Materials **4**(1), 1994, pp. 35–41.

[8] GOLDNER P., PELLÉ F., *Photon avalanche fluorescence and lasers*, Optical Materials **5**(4), 1996, pp. 239–249.

[9] AUZEL F., *Upconversion processes in coupled ion systems*, Journal of Luminescence **45**(1–6), 1990, pp. 341–345.

[10] AUZEL F., YIHONG CHEN, *Photon avalanche luminescence of Er^{3+} ions in $LiYF_4$ crystal*, Journal of Luminescence **65**(1), 1995, pp. 45–56.

[11] BOULMA E., JOUART J.P., BOUFFARD M., DIAF M., DOUALAN J.L., MONCORGÉ R., *Laser-induced, Er^{3+} trace-sensitized red-to-blue photon-avalanche up-conversion in Tm^{3+}:KY_3F_{10}*, Optical Materials **30**(7), 2008, pp. 1028–1032.

[12] BRENIER A., GARAPON C., MADEJ C., PEDRINI C., BOULON G., *Influence of looping mechanisms in up-conversion processes in Yb–Tm–Ho doped $Gd_3Ga_5O_{12}$*, Journal de Physique IV **4**(C4), 1994, p. C4-431.

[13] RUBIN J., BRENIER A., MONORGÉ R., PEDRINI C., MOINE B., BOULON G., ADAM J.L., LUCAS J., HENRY J.Y., F*luorescence dynamics in some solid-state laser materials emitting in the infrared region: Ho^{3+} doped $LiYF_4$ single crystals and fluoride glasses*, Journal de Physique Colloques **48**(C7), 1987, p. C7-367.

[14] BRENIER A., RUBIN J., MONCORGÉ R., PEDRINI C., *Excited-state dynamics of the Tm^{3+} ions and $Tm^{3+} \rightarrow Ho^{3+}$ energy transfers in $LiYF_4$*, Journal de Physique **50**(12), 1989, pp. 1463–1482.

[15] ALLAIN J.Y., MONERIE M., POIGNANT H., *Tunable green upconversion erbium fibre laser*, Electronics Letters **28**(2), 1992, pp.111–113.

[16] CONGSHAN ZHU, XIAOJUAN LU, ZUYI ZHANG, *Upconversion fluorescence of TeO_2–PbO-based oxide glasses containing Er^{3+} ions*, Journal of Non-Crystalline Solids **144**, 1992, pp. 89–94.

[17] VETRONE F., BOYER J.C., CAPOBIANCO J.A., SPEGHINI A., BETTINELLI M., *980 nm excited upconversion in an Er-doped ZnO–TeO_2 glass*, Applied Physics Letters **80**(10), 2002, p. 1752.

[18] HAI LIN, GERALD MEREDITH, SHIBIN JIANG, XIANG PENG, TAO LUO, NASSER PEYGHAMBARIAN, EDWIN YUE-BUN PUN, *Optical transitions and visible upconversion in Er^{3+} doped niobic tellurite glass*, Journal of Applied Physics **93**(1), 2003, pp. 186–191.

[19] FENG SONG, MYERS M.J., SHIBIN JIANG, YAN FENG, CHEN X.B., GUANGYIN ZHANG, *Effect of erbium concentration on upconversion luminescence of Er:Yb:phosphate glass exited by InGaAs laser diode*, Proceedings of SPIE **3622**, 1999, pp. 182–188.

[20] HONGPING MA, SHIQING XU, *Effect of GeO_2 content on upconversion luminescence of Er^{3+}-doped PbF_2–SiO_2–GeO_2 glassses*, Journal of Materials Science **41**(10), 2006, pp. 3155–3157.

[21] LIAO M., HU L., DUAN Z., ZHANG L., WEN L., *Spectroscopic properties of fluorophosphates glass with high Er^{3+} concentration*, Applied Physics B: Lasers and Optics **86**(1), 2007, pp. 83–89.

[22] ZHANG X., JOUART J.P., MARY G., LIU X., YUAN J., *Red excited-state absorption and up-conversion in Er^{3+}:$Ca_3Al_2Ge_3O_{12}$*, Journal of Luminescence **72–74**, 1997, pp. 983–984.

[23] PETIT L., CARDINAL T., VIDEAU J.J., LE FLEM G., GUYOT Y., BOULON G., COUZI M., BUFFETEAU T., *Effect of the introduction of $Na_2B_4O_7$ on erbium luminescence in tellurite glasses*, Journal of Non-Crystalline Solids **298**(1), 2002, pp. 76–88.

[24] NINGNING ZU, HAIGUI YANG, ZHENWEN DAI, *Different processes responsible for blue pumped, ultraviolet and violet luminescence in high-concentrated Er^{3+}:YAG and low-concentrated Er^{3+}:YAP crystals*, Physica B: Condensed Matter **403**(1), 2008, pp. 174–177.

[25] CHEN G.Y., LIU Y., ZHANG Z.G., AGHAHADI B., SOMESFALEAN G., SUN Q., WANG F.P., *Four-photon upconversion induced by infrared diode laser excitation in rare-earth-ion-doped Y_2O_3 nanocrystals*, Chemical Physics Letters **448**(1–3), 2007, pp. 127–131.

[26] BRENIER A., *Laser-heated pedestal growth of Er^{3+}-doped Gd_2O_3 single crystal fibres and up-conversion processes*, Chemical Physics Letters **290**(4–6), 1998, pp. 329–334.

[27] TANABE S., SUZUKI K., SOGA N., HANADA T., *Mechanisms and concentration dependence of Tm^{3+} blue and Er^{3+} green up-conversion in codoped glasses by red-laser pumping*, Journal of Luminescence **65**(5), 1995, pp. 247–255.

[28] JUDD B.R., *Optical absorption intensities of rare-earth ions*, Physical Review **127**(3), 1962, pp. 750–761.

[29] OFELT G.S., *Intensities of crystal spectra of rare-earth ions*, Journal of Chemical Physics **37**(3), 1962, p. 511.

[30] JABA N., KANOUN A., MEJRI H., SELMI A., ALAYA S., MAAREF H., *Infrared to visible up-conversion study for erbium-doped zinc tellurite glasses*, Journal of Physics: Condensed Matter **12**(20), 2000, pp. 4523–4534.

[31] CANTELAR E., NEVADO R., LIFANTE G., CUSSO F., *Modelling of 980 nm pumped EDWAs: spectroscopic variations associated to fabrication process*, Optical and Quantum Electronics **33**(4–5), 2001, pp. 561–569.

[32] BERKDEMIR S., ÖZSOY S., *Schematic representations for teaching the procedure of optical amplification in fiber amplifiers*, Ref Etop083.

[33] DOS SANTOS E.A., COURROL L.C., KASSAB L.R.P., GOMES L., WETTERB N.U., VIEIRA N.D., RIBEIRO S.J.L., MESSADDEQ Y., *Evaluation of laser level populations of erbium-doped glasses*, Journal of Luminescence **124**(2), 2007, pp. 200–206.

[34] KACZMAREK F., KAROLCZAK J., *Infrared-to-visible upconversion in erbium fluoride (ZBLAN:Er^{3+}) optical fiber: competition between the parasitic 850-nm fluorescence and the green laser emission at 544 nm*, Opto-Electronics Review **12**(2), 2004, pp. 247–248.

[35] WU R., MYERS J.D., MYERS M.J., RAPP C.F., *Fluorescence lifetime and 980nm pump energy transfer dynamics in erbium and ytterbium co-doped phosphate laser glasses*, Proceedings of SPIE **4968**, 2003, pp. 11–17.

[36] TANGUY E., LARAT C., POCHOLLE J.P., *Modelling of the erbium–ytterbium laser*, Optics Communications **153**(1–3), 1998, pp. 172–183.

[37] TOMA O., GEORGESCU S., *Pump wavelengths for an upconversion-pumped Er:YAG green-emitting laser*, Optics-Lasers, 2005.

[38] MOINE B., BOURCET J.C., BOULON G., REISFELD R., KALISKY Y., *Interaction mechanisms in the Bi^{3+}–Eu^{3+} energy transfer in germanate glass at low temperature*, Journal de Physique **42**(3), 1981, pp. 499–503.

[39] SAVOINI B., MUÑOZ SANTIUSTE J.E., GONZÁLEZ R., *Optical characterization of Pr^{3+}-doped yttria-stabilized zirconia single crystals*, Physical Review B **56**(10), 1997, pp. 5856–5865.

[40] ROTMAN S.R., LURIA E., YITZHAKI N., EYAL A., *Practical models for energy transfer between ions in solids*, Optical Materials **5**(1–2), 1996, pp. 1–33.

Received January 26, 2009
in revised form April 22, 2009